Iron oxyhydroxide and sulphide mineralization in hydrocarbon seep-related carbonate submarine chimneys, Gulf of Cadiz (SW Iberian Peninsula)

R. Merinero [a,*], R. Lunar [a], J. Martínez-Frías [b], L. Somoza [c], V. Díaz-del-Río [d]

[a] Crystallography and Mineralogy Department, Universidad Complutense de Madrid (UCM), c/ José Antonio Novais 2, Ciudad Universitaria, 28040 Madrid, Spain
[b] Planetary Geology Laboratory, Centro de Astrobiología (CSIC/INTA), Associated to the NASA Astrobiology Institute, Crta. Ajalvir, km. 4, 28850 Torrejón de Ardoz, Madrid, Spain
[c] Marine Geology Division, Geological Survey of Spain (IGME), c/ Ríos Rosas 23, 28003 Madrid, Spain
[d] Malaga Oceanographic Centre, Instituto Español de Oceanografía (IEO), Apdo. 285, 29640 Fuengirola (Malaga), Spain

Keywords:
Gulf of Cadiz
Pyrite goethite framboid
Methane carbonate

A B S T R A C T

This paper aims to investigate the iron mineralization hosted in the submarine hydrocarbon seep-related carbonate chimneys, from the Gulf of Cadiz continental slope (SW Iberia). Chimneys are made of a general fine groundmass of major Fe-rich dolomite, ankerite and calcite, small grains of quartz and phyllosilicates, and some foraminifer tests and ostracod shells. Primary porosity is frequently generated inside foraminifer chambers and ostracod shells, and is filled with closely packed microcrystals of iron oxyhydroxide and sulphide minerals forming framboids. Some extremely peculiar multiframboidal textures are also detected, corresponding to microcrystal groups, spherical framboids and euhedral crystals without framboidal texture. The mineralogy observed is mainly goethite (pyrite pseudomorphs); traces of tiny grains of pyrite were also observed. Cubic, octahedral and pyritohedral are the habits observed in both minerals. Chemical analyses of framboids and euhedral crystals display high (often erratic) amounts of As, Co, Ni and Mo in oxyhydroxides and Mo, Pb, V and Co in sulphides versus almost always negligible concentrations of Cu and Zn. A textural, geochemical and mineralogical evolution is proposed to explain the coexistence of different morphologies in the multiframboidal texture: (a) growth and aggregation of microcrystals as typical framboidal-type mineralogical associations; (b) development of euhedral habits; (c) coalescence and homogenization of the microcrystal into large size (euhedral to anhedral) crystals, and (d) formation of euhedral crystals or polycrystalline masses, with complete loss of framboidal texture. Along this process, an increase of the concentration of Fe, S, Mn and Ti, linked to a decrease in Mg, Si, Al, As, P, Ca and V was observed. The study of the iron mineralization in the Gulf of Cadiz is a first, and can give clues to understand the complex geobiological interactions in this and other similar extreme hydrocarbon-bearing submarine ecosystems.

1. Introduction

Marine cold seeps and methane vents are common features of continental margins and other geodynamic settings worldwide (see Paull and Neumann, 1987; Brooks et al., 1991; Ivanov et al., 1991; Whiticar and Werner, 1991; Jørgensen, 1992; Laier et al., 1992; De Angelis et al., 1993; Dando et al., 1994; Paull et al., 1995; Boehme et al., 1996; Cable et al., 1997; Orpin, 1997; Stakes et al., 1999; DeLong, 2000; Paull et al., 2005, among others) with no elevated temperatures, where methane-rich fluids flow through the continental crust and are colonized by large communities of microbial and chemosynthetic organisms. Methane is generated from various sources: thermogenic and biogenic methane and decomposing methane hydrates, and is seeping to the hydrosphere and potentially to the atmosphere. Cold seeps are associated with authigenic carbonates building chemoherms (e.g. Bohrmann et al., 1998, 2002; Suess et al., 1998; Naehr et al., 2000; Pierre et al., 2000; Peckmann et al., 2001; Thiel et al., 2001; Aloisi et al., 2002; Hübscher and Kukowski, 2003; Han et al., 2004; Teichert et al., 2005, among others) that resemble reefs and/or chimneys (Shnukov et al., 1995; Orpin, 1997; Stakes et al., 1999; Michaelis et al., 2002; Gulin et al., 2003).

Iron sulphide precipitation is often associated with these microbially mediated carbonates. The anaerobic oxidation of methane (AOM) in anoxic marine sediments is directly linked to sulphate reduction (Barnes and Goldberg, 1976; Nauhaus et al., 2002; Valentine, 2002), through a syntrophic interaction between methanogenic archaea and sulphate-reducing bacteria (e.g. Hoehler et al., 1994; Elvert et al., 1999, 2000; Hinrichs et al., 1999, 2000; Thiel et al., 1999, 2001; Boetius et al., 2000; Pancost et al., 2000, 2001;

* Corresponding author. Tel.: +34 1 3944959; fax: +34 1 3944872.
E-mail address: rmeriner@geo.ucm.es (R. Merinero).

Table 1
Major and trace element analyses of carbonate chimney samples (results are in ppm)

Sample	Si	Al	Fe	Ca	Ti	Mn	K	Mg	P	Na	Sr	Ba	V	As	Zr	Cr	Zn	Ni	Sc	Rb	Co
10SN0004-AN00	58909	21117	96 403	183 325	1415	736	6400	55733	1881	9132	492	162	222	143	73	62	74	48	31	27	40
10SN0005-AN00	45 735	16671	103 754	180224	1073	596	4707	65164	1589	7129											
01010007-AN01	40 083	17 624	98 109	174620	1061	929	4740	75 373	1471	5430	386	128	232	147	53	43	60	40	31	23	41
02260011-AN01	44 660	18312	51 617	191640	1079	604	5122	82801	1296	5297	892	267	147	85	46	53	42	27	29	26	14
18220018-AN01	106 471	22706	32679	193482	1205	263	5919	49 143	2117	2381	990	117	80	53	72	54	28	17	31	28	4
15070093-AN01	92 829	32 550	59090	172 783	1283	612	6152	51954	1942	4518	552	165	118	74	82	75	37	26	27	28	19

Valentine and Reeburgh, 2000; Bian et al., 2001; Lanoil et al., 2001; Orphan et al., 2001, 2002; Thomsen et al., 2001; Hinrichs and Boetius, 2002; Michaelis et al., 2002; Teske et al., 2002; Zhang et al., 2002). This biogeochemical process is represented by the net reaction:

$$CH_4 + SO_4^{2-} \rightarrow HCO_3^- + HS^- + H_2O$$

In marine methane seeps, the process of AOM and resulting HCO_3^- production is thought to foster carbonate formation through localized increases in alkalinity (e.g. Ritger et al., 1987; Paull et al., 1992; Sassen et al., 2004). Hydrogen sulphide can combine with iron and other elements retained in walls and covers of bacteria cells, favouring the precipitation of pyrite and other iron sulphides. Framboidal texture (basically a spherical packed aggregate of microcrystals) is one of the principal occurrences of pyrite in sedimentary environments (Chauhan, 1974; Elverhoi, 1977; Sawlowicz, 1993; Wilkin and Barnes, 1997; Butler and Rickard, 2000; Schoonen, 2004). Pyrite, as well as other iron sulphides and oxyhydroxides, presents framboidal texture in a broad range of conditions, from hydrothermal deposits (Martínez-Frías et al., 1997) to magmatic (Love and Amstutz, 1969) and metamorphic rocks (Schieber and Baird, 2001; Boyle et al., 2003), even in ancient books and fossil wood (García-Guinea et al., 1997, 1998). Pyrite framboids often occur in close spatial relationship with organic matter, silica or carbonates, which influence their formation and growth, containing organic matter both in their interstices and/or as membranes coating framboids (Love and Amstutz, 1966; Sweeney and Kaplan, 1973; Taylor, 1982; Sawlowicz, 2000).

The term "polyframboid" was suggested by Love (1971) and represents aggregates of framboid units with the same size. Multiframboids are more complex textures (Massaad, 1974; Roberts et al., 2005; Merinero et al., 2005, 2006), characterized by a mixture of crystal sizes and morphologies (microcrystals, subspherical framboids and euhedral crystals). Availability of space and nutrients (sulphur, iron and other metals) are necessary for the polyframboid formation.

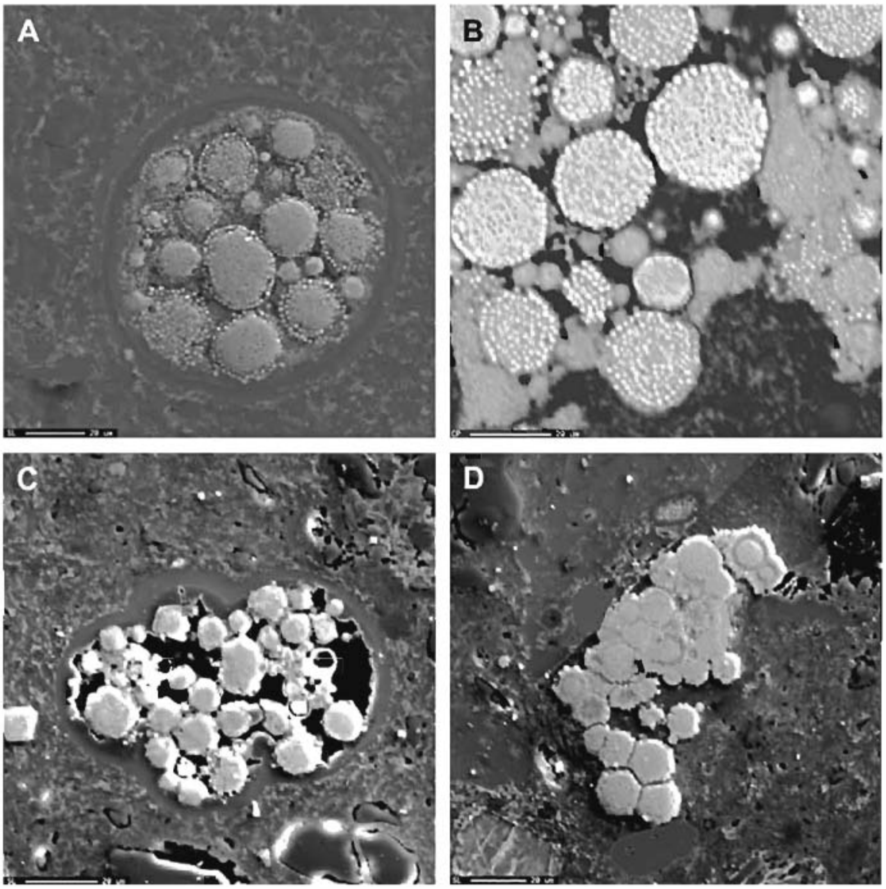

Fig. 1. BSE images of thin sections. (A) and (B) subspherical framboids with microcrystal arrangement. (C) and (D) euhedral morphologies with internal framboidal texture.

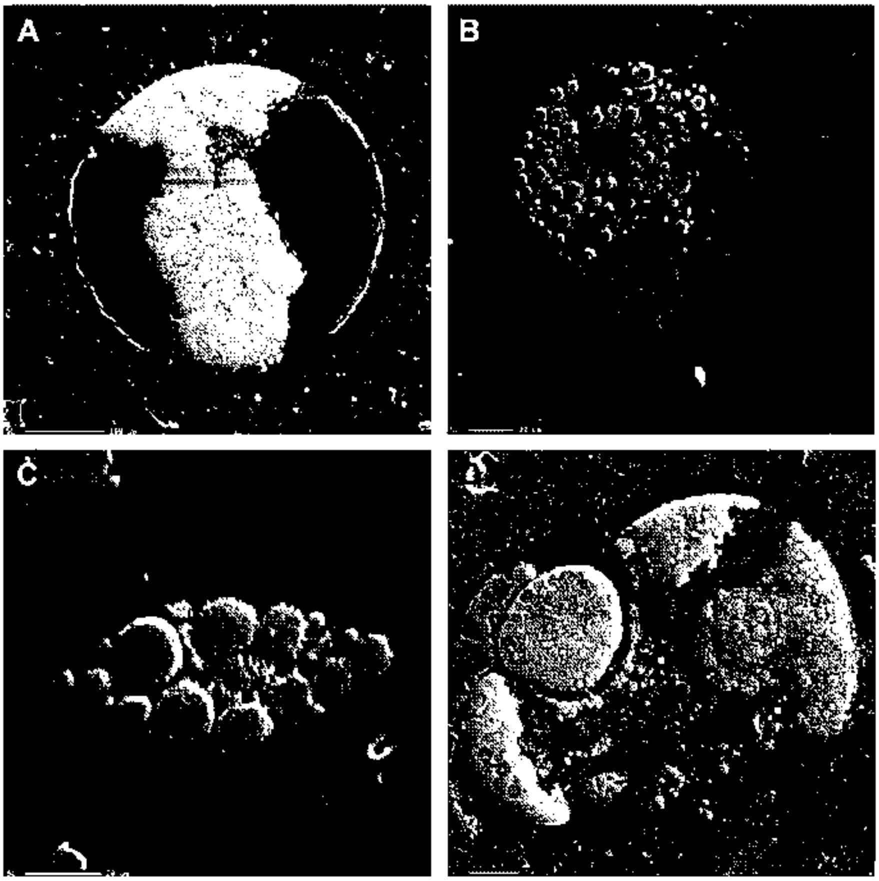

Fig. 2. BSE images of thin sections of framboids filling foraminifer tests. Primary porosity generated inside foraminifer tests (A, B and D) and ostracod shells (C) are the main sites where microcrystal aggregates forming spherical framboids are found. Prismatic crystals can grow rimming framboids (A). Organic matter and clay minerals inclusions parallel to the crystal faces are formed in euhedral morphologies (B).

The Gulf of Cadiz (SW Iberia) contains active hydrocarbon-rich vents (Somoza et al., 2003), extensive mud volcanism, mud diapirism and authigenic carbonates (chimneys, slabs and crusts) with light carbon isotopes' compositions. These features have been interpreted as indicators of the existence of reduced compounds (particularly methane and hydrogen sulphide) on or immediately below the seafloor (Díaz-del-Río et al., 2003). Since the discovery of the carbonate chimneys in 2000 (Díaz-del-Río et al., 2001), main studies are concentrated on the possible genesis of these carbonate structures. The present article is particularly focussed on the study of iron mineralization, trying to determine its role in the general process of formation of the chimneys, as well as to understand the complex geobiological interactions in this and other similar extreme hydrocarbon-bearing submarine ecosystems.

2. Materials and methods

Samples were taken with a rectangular benthic-type dredge at mounds on the Gulf of Cadiz continental slope during 2000 and 2001 R/V Cornide de Saavedra cruises. A BENTHOS underwater camera was used to obtain bottom photographs. More than 200 carbonate chimneys were collected from four sites at depths ranging from 850 to 1100 m (ANAS00-DA10: 36°8′ N/7°43′ W; ANAS01-DA1: 36°06.96′ N/7°36.31′ W; DA2: 36°06.48′ N/7°36.93′ W; DA15: 36°09.29′ N/7°32.89′ W and DA18: 36°09.29′ N/7°32.89′ W). Further details can be found in Díaz-del-Río et al. (2003). Chimneys show a wide variety of shapes and range in size from several centimetres to a few decimetres and consist of porous fine-grain carbonates (mainly Fe-rich dolomite) hosting quartz grains, Fe–Ti oxides and phyllosilicate grains, foraminifer tests and ostracod shells as main components.

From a set of 24 chimneys, six representative specimens were selected for the analyses. Bulk mineralogy was determined using X-ray diffraction (XRD) on powder samples using a diffractometer with Cu Kα radiation (Philips PW-1700). Phillips ADP program and ICDD database are used for mineral identification. The geochemical composition of the bulk rock (major, minor and trace elements) was analysed by X-ray fluorescence using a spectrometer MagiX of PANanalytical with Rh tube and software X-40.

In addition to the conventional study of thin and polished sections by transmitted and reflected light optic microscopy, a textural, compositional and mineralogical investigation of the samples was made using a Philips XL20 scanning electron microscope with accelerating voltages of 20–30 kV and an electron microprobe WDS (EPMA, Electron Probe Micro Analyzer) JEOL mark and Superprobe JXA-8900M model (Electron Microscopy Centre "Luis Bru", Complutense University of Madrid). It is equipped with four wavelength dispersion spectrometers (four canals) where the following crystals are lodged: Channel 1, TAP and LDE2; Channel 2, PETJ and LIF; Channel 3, PETJ and LIF; Channel 4, PETJH and LIFH. A total of 250 punctual analyses were made with a difference of potential of 20 kV, a current intensity of 50 nA, with focussed beam and variable measure times, according to different elements, from 10 to 20 s in the sharp point, and from 5 to 10 s in the background point. The corrections of the intensities were made with ZAF matrixes.

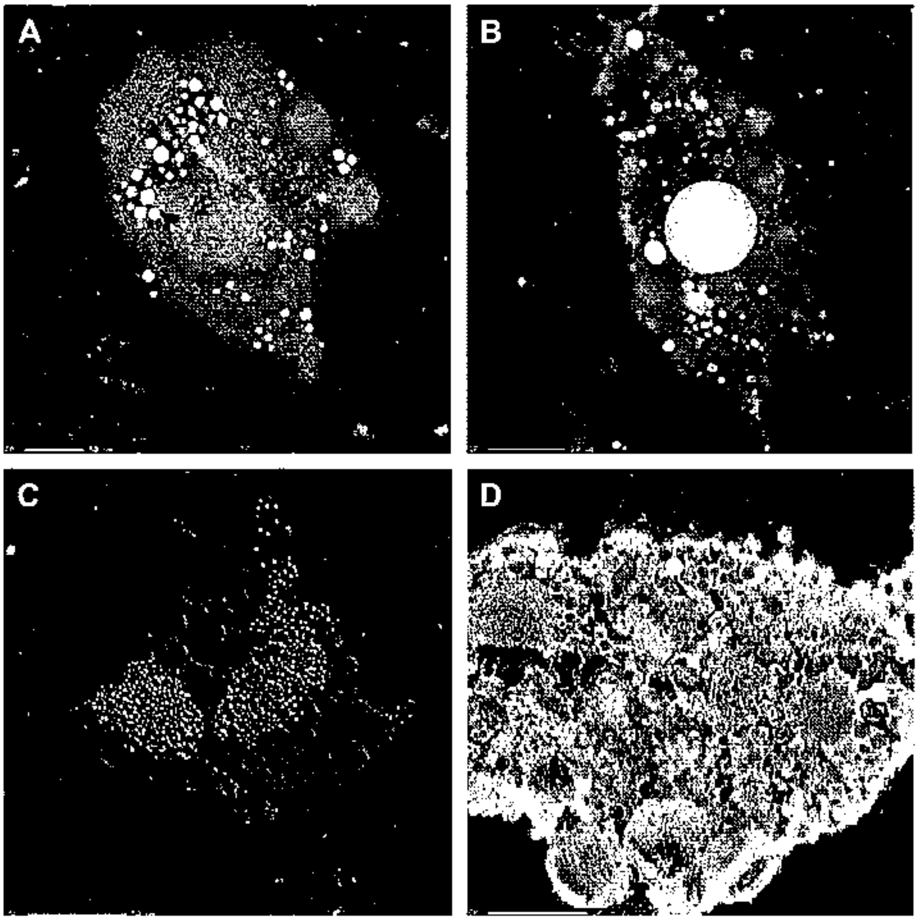

Fig. 3. BSE images of thin sections of multiframboidal textures. Irregular and spherical packets of microcrystal and euhedral crystal with or without framboidal texture can be observed in multiframboidal textures.

3. Results and discussion

The carbonate chimneys which host the iron mineralization are mainly composed by Fe-rich dolomite and ankerite trace amounts of quartz, calcite and goethite were also detected. The whole-rock geochemistry of carbonate chimneys is summarized in Table 1.

3.1. *Iron mineralization: mineralogy and textures*

Primary porosity generated inside foraminifer chambers and ostracod shells often is filled with closely packed microcrystals of iron minerals forming framboids. Different morphologies are observed: from irregular morphologies and subspherical associations of microcrystals (framboids sensu stricto) to subeuhedral and euhedral crystals with or without internal microcrystals (Figs. 1 and 2). In addition, multiframboidal textures are also found in the samples: mainly, groups of microcrystals, spherical framboids and euhedral crystals (Fig. 3). Microcrystals and euhedral crystals show cubic, octahedral and pyritohedral habits. Goethite is the principal mineral of the framboids and euhedral morphologies, and only one sample (sample 18220018-AN01) shows both goethite and pyrite forming framboids and euhedral crystals (Fig. 4). In this sample, the contents in Fe, V, Ba, Mn, As, Zn, Ni and Co are the lowest, and contents in Si, Ca, P and Sr are the highest (Table 1) with respect to the whole set of chimneys analysed.

In accordance with the well-known 'Ostwald rule', for low temperatures, framboidal pyrite growth is usually preceded by the formation of unstable iron monosulphides mackinawite (FeS) and greigite (Fe_3S_4), the least stable sulphide precipitating first (Rickard et al., 1995; Wilkin and Barnes, 1997). Transformation from greigite to pyrite may occur either by sulphur addition (Berner, 1984) or iron loss (Furukawa and Barnes, 1995) preserving the framboidal morphology.

Although few works are published about framboidal oxy-hydroxides (Mucke et al., 1999) oxidation of framboidal pyrite is a common process (Luther et al., 1982; Wilkin and Barnes, 1997). Pyrite oxidation studies (Huggins et al., 1980) showed that pyrite transforms first into szomolnokite ($FeSO_4 \cdot H_2O$), then oxidizes to lepidocrocite (α-FeO(OH)), and passes finally to goethite (γ-FeO(OH)). The oxyhydroxide habits, and its coexistence with iron sulphides in the same foraminifer remains in sample 18220018-AN01 (Fig. 4), suggest goethite formation as the result of pseudomorphism after pyrite.

3.2. *Crystal and framboid sizes*

The dimension of 196 framboids and euhedral crystals was measured, with special attention to microcrystal, framboid and multiframboid sizes and the different crystal morphologies (see Table 2). Most framboids range from 5 to 20 μm in size (Wilkin et al., 1996), although framboids as large as 250 μm have occasionally been found (Sweeney and Kaplan, 1973). In our case, we have detected that the different scales of size and complexity of framboidal morphologies are related, as previously defined, to a continuous growth and rearrangement of framboids into euhedral crystals. Thus, in accordance with Sawlowicz (1993), euhedral

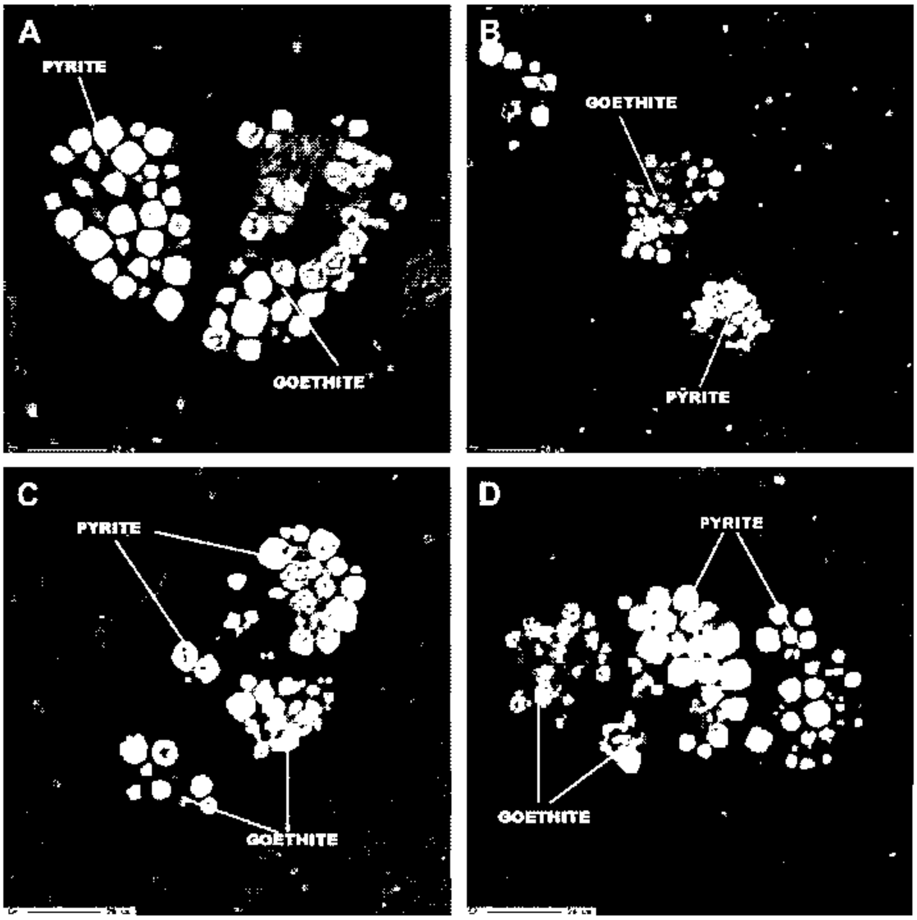

Fig. 4. BSE images of thin sections. Pyrite and goethite coexistence in the same foraminifer test. Crystals filling foraminifer tests have different mineral composition, but a chamber presents always the same mineralogy.

crystals are much more easily formed from microcrystals and framboids of small sizes than from multiframboid and large framboids, which explains the significant size differences with respect to the observed morphologies.

3.3. *Iron minerals geochemistry*

Framboidal and euhedral goethite and pyrite were analysed by electron microprobe (see Section 2), paying special attention to crystal morphologies (Table 3). Mg, Si, Al, Ca and P anomalies detected can be interpreted in connection with the existence of fine-grain carbonates, clay minerals and organic matter filling interstices in the framboids. The small grain size of the microcrystals (in our case, 143 nm of mean size) and the large effective surface of framboids make effective the adsorption of dissolved cations and inorganic anions, organic matter with fine-grain materials, iron oxides and clay minerals. As it has been demonstrated (Morse et al., 1987), adsorption or co-precipitation reactions play an important role in the control of trace metal concentrations in anoxic environments. Especially significant is the large concentration of Mo found in sulphide crystals. Mo is very mobile in the upper portion of the anoxic sediments, but is fixed in iron sulphides at depth (Malcom, 1985), but it is released during the transformation of monosulphides to pyrite. The presence of large concentrations of Mo in framboidal and euhedral pyrite (more than 11 000 ppm) is indicative of the possible existence of previous monosulphides phases (mackinawite and greigite) in the pyrite formation. Many trace metals have been found to be frequently associated with iron sulphides in anaerobic environments, including Zn, Pb, Co, Ni, As and occasionally Mn. The association of the different trace metals varies in different environments. Ni and Co are strongly associated with sulphides, while Zn and Mo were

Table 2
Statistical data for crystal sizes measured in different crystal morphologies

	N	Mean (μm)	Measured error (μm)	Minimum (μm)	Maximum (μm)	Standard deviation
Microcrystals	106	1.4	±0.15	0.8	3.5	0.55
Framboids	196	21.3	±0.28	5.5	59.1	12.79
Multiframboid	157	131.8	±0.62	9.5	297.5	118.05
Irregular	11	37.5	±3.07	18.6	56.1	10.19
Subspherical	35	23.6	±2.05	7.5	59.1	12.15
Subeuhedral	46	22.6	±1.58	9.2	49.0	10.72
Euhedral with microcrystals	26	25.3	±1.94	5.5	50.9	9.89
Euhedral without microcrystals	68	14.1	±0.97	5.9	48.3	7.97

Table 3
Electron microprobe analyses comparison between subeuhedral–euhedral and subspherical–irregular morphologies and pyrite and goethite crystals (results are in ppm)

Morphology	Mg	Si	Al	As	P	Ca	V	Ni	Mo	Co	Pb	Fe	S	Mn	Ti	Zn
Subspherical–irregular	11629	7903	6005	1974	5724	7019	751	323	380	745	528	574613	287	569	246	393
Subeuhedral–euhedral	10205	6728	5136	1227	5013	6589	508	271	360	729	514	581417	403	671	306	402
Difference	1423	1175	869	747	711	430	243	52	20	17	14	−6804	−117	−102	−60	−9
Pyrite	1546	1726	909	403	388	6708	1376	–	11024	477	3395	506115	469437	209	127	268
Goethite	14897	9637	2801	2246	5338	11989	812	282	329	674	677	604146	1678	323	137	321
Difference	13351	7911	1892	1843	4950	5281	564	282	10695	197	2718	98031	467759	114	10	54

more strongly bound by organic matter. As is specially associated with framboidal and noneuhedral pyrite (Graham and Robertson, 1995; Ratnamohan et al., 1998). In the samples analysed Mo, Pb and V are preferably associated with iron sulphides, and the other hand, As, Co, Mn and Zn are associated to iron oxyhydroxides (Table 3).

3.4. Framboidal evolution

Close spatial relationship between framboidal and euhedral was often observed in nature and suggests genetic relationship (Love, 1965; Kalliokoski, 1965; Love and Amstutz, 1966; Ostwald and England, 1977, 1979; Swalowicz, 1987, 1993). Multi-faceted framboids with regular arrangement of microcrystals represent the link between these two morphologies (Sawlowicz, 1993). Love and Amstutz (1966) suggested the possibility of recrystallization from framboidal to single grain pyrite. Sawlowicz (1993) developed this suggestion and proposed a continuous growth of microcrystals in the framboids (sometimes towards euhedral crystals) as long as they are in contact with the initial solution. Martínez-Frías et al. (1997) defined a textural evolution pattern where framboids are progressively better faceted until they become euhedral in morphology. In the iron mineralization of the chimneys, some intermediate steps of this pattern occur, characterized by: (a) irregular morphologies (before framboid formation) and (b) microcrystal arrangement and lose of framboidal texture (before transformation into euhedral crystals).

Although framboidal pyrite can be synthesized inorganically (Farrand, 1970; Butler et al., 2000), in natural sediments the chemical environment that is necessary for the formation of iron sulphides is created by sulphate-reducing bacteria activity (Berner, 1984). As indicated before, the growth and aggregation of microcrystals in framboidal-type associations represent the first stage of evolution, with formation of irregular morphologies and spherical framboids. Further development of cubic, octahedral and pyritohedral habits is represented by subeuhedral morphologies and multi-faceted framboids (Fig. 5). Differentiation (or loss) of organic matter in internal crystal inclusions also occurs. This is significant, as final euhedral crystals are formed with complete loss of the framboidal texture and the expulsion of organic matter occupying interstitial sites (in many cases, organic matter inclusions parallel to the crystal faces are formed). Of course, it is also plausible that euhedral pyrite not always formed via framboid evolution, and, therefore, direct precipitation cannot be excluded. It is important to stress that in sites with availability of space, large size foraminifer chambers and porosity generated between clasts, multiframboidal textures are observed, and all the stages of textural evolution can be found. A continuous activity of sulphate-reducing bacteria, the iron and space availability as well as the textural evolution could explain this coexistence.

Regarding the chemical element variations (Table 3), there are significant high concentrations of Fe, S, Mn and Ti and low concentrations of Mg, Si, Al, As, P, Ca and V in subeuhedral and euhedral morphologies in comparison with subspherical and irregular morphologies. These differences could be explained as a consequence of expulsion and differentiation of fine-grain carbonates, organic matter and clay elements during framboidal recrystallization.

4. Conclusions

The study of iron oxyhydroxide and sulphide mineralization occurred in hydrocarbon seep-related carbonate submarine chimneys of the Gulf of Cadiz reveals the presence of a great variety of morphologies, textures, mineralogy and geochemical concentrations.

Textural evolution (Fig. 5) consists of faces development with progressive loss of internal framboidal texture and microcrystal size increase. Growth of prismatic crystals rimming the framboids and formation of concentric inclusions of organic matter and clay minerals also occurred. The different scales of size and complexity of framboidal morphologies are related to a continuous growth and rearrangement of framboids into euhedral crystals. Geochemical changes are linked to the textural evolution. Expulsion and differentiation of fine-grain carbonates, organic matter and clay elements during framboidal recrystallization causes a decrease in Mg,

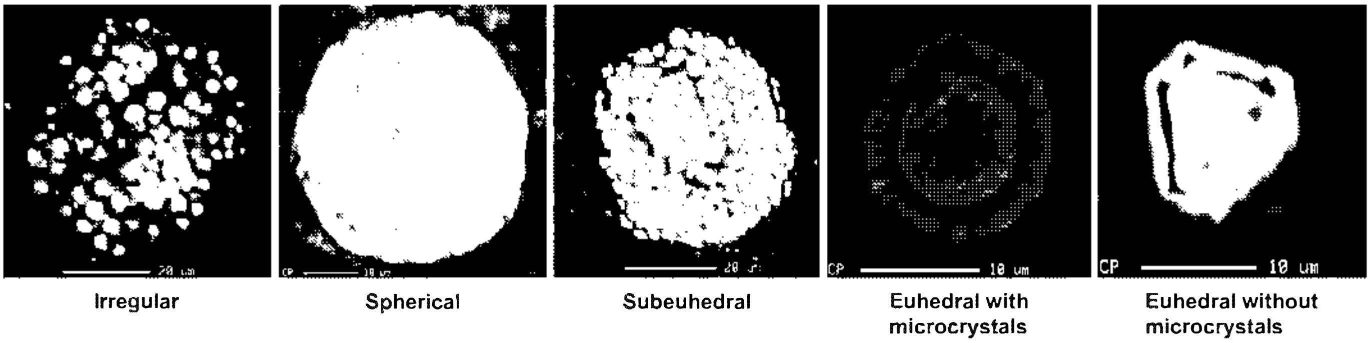

Fig. 5. Textural evolution proposed by the authors: irregular and spherical microcrystals packing, faces development with subeuhedral and euhedral textures with internal framboidal texture, and finally faceted crystals with loss of framboidal texture, and development, in many cases, of inclusions parallel to crystal faces (BSE images of thin sections).

Si, Al, As, P, Ca and V concentrations with increase in Fe, S, Mn and Ti.

Iron oxyhydroxides' habits and the coexistence with sulphide crystals in the same sample are interpreted as a process of pseudomorphism of goethite after pyrite with framboidal texture preservation and redistribution of some elements could take place. Large concentrations of Mo in framboidal and euhedral pyrite could be related with previous monosulphides phases.

Sulphate-reducing bacteria activity is the principal way that provides geochemical conditions for iron sulphide precipitation in sedimentary environments with lower concentrations of oxygen (Berner, 1984). Thus, in the Gulf of Cadiz formation of authigenic carbonates and iron minerals filling porosity could be signals of anaerobic oxidation of methane and bacterial sulphate reduction. Likewise, the presence of multiple morphologies in the same sample, even in the same multiframboidal texture suggests a link between mineral evolution, iron and space availability and microorganisms activity.

References

Aloisi, G., Bouloubassi, I., Heijs, S.K., Pancost, R.D., Pierre, C., Damsté, J.S.S., Gottschal, J.C., Forney, L.J., Rouchy, J.-M., 2002. CH_4-consuming microorganisms and the formation of carbonate crusts at cold-seeps. Earth and Planetary Science Letters 203, 195–203.

Barnes, R.O., Goldberg, E.D., 1976. Methane production and consumption in anoxic marine sediments. Geology 4, 297–300.

Berner, R.A., 1984. Sedimentary pyrite formation: an update. Geochimica et Cosmochimica Acta 48, 605–615.

Bian, L., Hinrichs, K.-U., Xie, T., Brassell, S.C., Iversen, N., Fossing, H., Jørgensen, B.B., Hayes, J.M., 2001. Algal and archaeal polyisoprenoids in a recent marine sediment: molecular isotopic evidence for anaerobic oxidation of methane. Geochemistry, Geophysics and Geosystems 2, doi:10.1029/2000GC000112.

Boehme, S.E., Blair, N.E., Chanton, J.P., Martens, C.S., 1996. A mass balance of ^{13}C and ^{12}C in an organic-rich methane-producing marine sediment. Geochimica et Cosmochimica Acta 60, 3835–3848.

Boetius, A., Ravenschlag, K., Schubert, C.J., Rickert, D., Widdel, F., Gieseke, A., Amann, R., Jørgensen, B.B., Witte, U., Pfannkuche, O., 2000. A marine microbial consortium apparently mediating anaerobic oxidation of methane. Nature 407, 623–626.

Bohrmann, G., Greinert, J., Suess, E., Torres, M.E., 1998. Authigenic carbonates from the Cascadia subduction zone and their relation to gas hydrate stability. Geology 26, 647–650.

Bohrmann, G., Suess, E., Greinert, J., Teichert, B., Naehr, T., 2002. Gas hydrate carbonates from Hydrate Ridge, Cascadia convergent margin: indicators of near-seafloor clathrate deposits. In: Proceedings of the Fourth International Conference on Gas Hydrates, Yokohama, pp. 102–107.

Boyle, A.P., Freitag, K., Nelson, E., Hitzman, M., Churchill, J., Lopez Pedrosa, M., 2003. Low Grade Metamorphism and Deformation of Pyrite in the Greens Creek Massive Sulphide Deposit, Admiralty Island, Alaska. Metamorphic Studies Group Research in Progress and Annual General Meeting. The Geological Society Burlington House, London (Abstract).

Brooks, J.M., Field, M.E., Kennicutt II, M.C., 1991. Observations of gas hydrates in marine sediments, offshore Northern California. Marine Geology 96, 103–109.

Butler, I., Rickard, D., 2000. Framboidal pyrite formation via the oxidation of iron (II) monosulfide by hydrogen sulphide. Geochimica et Cosmochimica Acta 64, 2665–2672.

Butler, I., Rickard, D., Grimes, S., 2000. Framboidal pyrite: self organisation in the Fe-S system. Goldschmidt. Journal of Conference Abstracts 5, 276–277.

Cable, J.E., Burnett, W.C., Chanton, J.P., 1997. Magnitude and variations of ground water seepage along a Florida marine shoreline. Biogeochemistry 38, 189–205.

Chauhan, D.S., 1974. Diagenetic pyrite from the lead–zinc deposits of Zawar, India. Mineralium Deposita 9, 69–73.

Dando, P.R., O'Hara, S.C.M., Schuster, U., Taylor, L.J., Clayton, C.J., Baylis, S., Laier, T., 1994. Gas seepage from a carbonate-cemented sandstone reef on the Kattegat coast of Denmark. Marine and Petroleum Geology 11, 182–189.

De Angelis, M.A., Lilley, M.D., Olson, E.J., Baross, J.A., 1993. Methane oxidation in deep-sea hydrothermal plumes of the Endeavour Segment of the Juan de Fuca Ridge. Deep-Sea Research I 40, 1169–1186.

DeLong, E.F., 2000. Resolving a methane mystery. Nature 407, 577–579.

Díaz-del-Río, V., Somoza, L., Martínez-Frías, J., Hernández-Molina, F.J., Lunar, R., Fernández-Puga, M.C., Maestro, A., Terrinha, P., Llave, E., García, A., García, A.C., Vázquez, J.T., 2001. Carbonate chimneys in the Gulf of Cadiz: initial report of their petrography and geochemistry. In: Final Proceedings of the International Conference of Geological Processes on Deep-Water European Margins, Moscow, Russia. UNESCO IOC Workshop Report 175, pp. 53–54.

Díaz-del-Río, V., Somoza, L., Martínez-Frías, J., Mata, M.P., Delgado, A., Hernández-Molina, F.J., Lunar, R., Martín-Rubí, J.A., Maestro, A., Fernández-Puga, M.C., León, R., Llave, E., Medialdea, T., Vázquez, J.T., 2003. Vast fields of hydrocarbon-derived carbonate chimneys related to the accretionary wedge/olistostrome of the Gulf of Cádiz. Marine Geology 195, 177–200.

Elverhoi, A., 1977. Origin of framboidal pyrite in clayey Holocene sediments and in Jurassic black shale in the northwestern part of the Barents Sea. Sedimentology 24, 591–595.

Elvert, M., Suess, E., Whiticar, M.J., 1999. Anaerobic methane oxidation associated with marine gas hydrates: superlight C-isotopes from saturated and unsaturated C_{20} and C_{25} irregular isoprenoids. Naturwissenschaften 86, 295–300.

Elvert, M., Suess, E., Greinert, J., Whiticar, M.J., 2000. Archaea mediating anaerobic methane oxidation in deep-sea sediments at cold seeps of the eastern Aleutian subduction zone. Organic Geochemistry 31, 1175–1187.

Farrand, M., 1970. Framboidal sulphides precipitated synthetically. Mineralium Deposita 5, 237–247.

Furukawa, Y., Barnes, H.L., 1995. Reactions forming pyrite from precipitated amorphous ferrous sulphide. In: Vairavamurthy, M.A., Schoonen, M.A.A. (Eds.), Geochemical Transformations of Sedimentary Sulphur. American Chemical Society Symposium Series, vol. 12, pp. 194–205.

García-Guinea, J., Martínez-Frías, J., González-Martín, R., Zamora, L., 1997. Framboidal pyrites in antique books. Nature 388, 631.

García-Guinea, J., Martínez-Frías, J., Harffy, M., 1998. Cell hosted pyrite framboids in fossil woods. Naturwissenschaften 85, 1–5.

Gulin, S.B., Polikarpov, G., Egorov, V., 2003. The age of microbial carbonate structures grown at methane seeps in the Black Sea with an implication of dating of the seeping methane. Marine Chemistry 84, 67–72.

Graham, U.M., Robertson, J.D., 1995. Micro-PIXE analysis of framboidal pyrite and associated maceral types in oil shale. Fuel 74, 530–535.

Han, X., Suess, E., Sahling, H., Wallmann, K., 2004. Fluid venting activity on the Costa Rica margin: new results from authigenic carbonates. International Journal Earth Sciences 93, 596–611.

Hinrichs, K.-U., Boetius, A., 2002. The anaerobic oxidation of methane: new insights in microbial ecology and biogeochemistry. In: Wefer, G., Billett, D., Hebbeln, D., Jørgensen, B.B., Schlüter, M., Van Weering, T. (Eds.), Ocean Margin Systems. Springer Verlag, Berlin, pp. 457–477.

Hinrichs, K.-U., Hayes, J.M., Sylva, S.P., Brewer, P.G., DeLong, E.F., 1999. Methane-consuming archaebacteria in marine sediments. Nature 398, 802–805.

Hinrichs, K.-U., Summons, R.E., Orphan, V., Sylva, S.P., Hayes, J.M., 2000. Molecular and isotopic analysis of anaerobic methane oxidizing communities in marine sediments. Organic Geochemistry 31, 1685–1701.

Hoehler, T.M., Alperin, M.J., Albert, D.B., Martins, C.S., 1994. Field and laboratory studies of methane oxidation in an anoxic marine sediment: evidence for a methanogen-sulfate reducer consortium. Global Biogeochemical Cycles 8, 451–463.

Hübscher, C., Kukowski, N., 2003. Complex BSR pattern in the Yaquina Basin off Peru. Geo-Marine Letters 23, 91–101.

Huggins, F.E., Huffman, G.P., Kosmach, D.A., Lowenhaupt, D.E., 1980. Mössbauer detection of goethite (alfa FeOOH) in coal and its potential as an indicator of coal oxidation. International Journal of Coal Geology 1, 75–81.

Ivanov, M.V., Polikarpov, G.G., Lein, A.Yu., Galchenko, V.F., Egorov, V.N., Gulin, S.B., Gulin, M.B., Rusanov, I.I., Miller, Y.M., Kuptsov, V.I., 1991. Biogeochemistry of carbon cycle at the methane seeps of the Black Sea. Proceedings of Academy of Sciences of USSR 320, 1235–1240 (in Russian).

Jørgensen, N.O., 1992. Methane-derived carbonate cementation of marine sediments from the Kattegat, Denmark: geochemical and geological evidence. Marine Geology 103, 1–13.

Kalliokoski, J., 1965. Framboids: colloid-crystals of pyrite (abstract). Economic Geology 60, 1562.

Laier, T., Jørgensen, N.O., Burchard, B., Cederberg, T., Kuijpers, A., 1992. Accumulation and seepages of biogenic gas in northern Denmark. Continental Shelf Research 12, 1173–1186.

Lanoil, B.D., Sassen, R., La Duc, M.T., Sweet, S., Nealson, K.H., 2001. Bacteria and archaea physically associated with Gulf of Mexico gas hydrates. Applied and Environmental Microbiology 67, 5143–5153.

Love, L.G., 1965. Micro-organic material with diagenetic pyrite from the lower Proterozoic Mount Isa Shale and a Carboniferous shale. Proceedings of the Yorkshire Geological Society 35, 187–201.

Love, L.G., Amstutz, G.C., 1966. Review of microscopic pyrite from the Devonian Chattanooga Shale and Rammelsberg Banderz. Fortschritte der Mineralogie 43, 277–309.

Love, L.G., Amstutz, G.C., 1969. Framboidal pyrite in two andesites. Neues Jahrbuch für Mineralogie – Abhandlungen 3, 97–108.

Love, L.G., 1971. Early diagenetic polyframboidal pyrite, primary and redeposited, from the Wenlockian Denbigh Grit Group, Conway, North Wales, U.K. Journal of Sedimentary Petrology 41, 1038–1044.

Luther III, G.W., Giblin, A., Howarth, R.W., Ryans, R.A., 1982. Pyrite and oxidized iron mineral phases formed from pyrite oxidation in salt marsh and estuarine sediments. Geochimica et Cosmochimica Acta 46, 2665–2669.

Malcom, S.J., 1985. Early diagenesis of molybdenum in estuarine sediments. Marine Chemistry 16, 213–225.

Massaad, M., 1974. Framboidal pyrite in concretions. Mineralium Deposita 9, 87–89.

Martínez-Frías, J., Navarro, A., Lunar, R., 1997. First reference of pyrite framboids in a Hg–Sb mineralization: the Valle del Azogue mineral deposit (SE Spain). Neues Jahrbuch für Mineralogie – Abhandlungen 4, 175–184.

Merinero, R., Lunar, R., Martínez-Frías, J., Somoza, L., Díaz-del-Río, V., 2005. Biomineralizaciones multi-framboidales en chimeneas submarinas metanógenas (Golfo de Cádiz). Macla 3, 135–137.

Merinero, R., Lunar, R., Martínez-Frías, J., Somoza, L., Díaz-del-Río, V., 2006. Iron-rich coccoidal microcrystals and framboids in submarine, methane-derived carbonate chimneys (Gulf of Cadiz, SW Iberian Peninsula): mineralogy, textures and astrobiological relevance. Geophysical Research Abstracts 8, 01382.
Michaelis, W., Seifert, R., Nauhaus, K., Trude, T., Thiel, V., Blumenberg, M., Knittel, K., Gieseke, A., Peterknecht, K., Pape, T., Boetius, A., Amann, R., Jørgensen, B.B., Widdel, F., Pechmann, J., Pimenov, N.V., Gulin, M.B., 2002. Microbial reefs in the Black Sea fueled by anaerobic oxidation of methane. Science 297, 1013–1015.
Morse, J.W., Millero, F.J., Cornwell, J.C., Rickard, D., 1987. The chemistry of hydrogen sulphide and iron sulphide systems in natural waters. Earth-Science Reviews 24, 1–42.
Mucke, A., Badejoko, T.A., Akande, S.O., 1999. Petrographic-microchemical studies and origin of the Agbaja Phanerozoic Ironstone formation, Nupe Basin, Nigeria: a product of a ferruginized ooidal kaolin precursor not identical to the Minette-type. Mineralium Deposita 34, 284–296.
Naehr, T.H., Rodriguez, N.M., Bohrmann, G., Paull, C.K., Botz, R., 2000. Methane-derived authigenic carbonates associated with gas hydrate decomposition and fluid venting above the Blake Ridge Diapir. In: Paull, C.K., Matsumoto, R., Wallace, P.J., Dillon, W.P. (Eds.), Proceedings of the Ocean Drilling Program. Scientific Results, vol. 164. Ocean Drilling Program, College Station, Texas, pp. 285–300.
Nauhaus, K., Boetius, A., Krüger, M., Widdel, F., 2002. In vitro demonstration of anaerobic oxidation of methane coupled to sulphate reduction in sediment from a marine gas hydrate area. Environmental Microbiology 4, 296–305.
Orphan, V.J., House, C.H., Hinrichs, K.-U., McKeegan, K.D., DeLong, E.F., 2001. Methane-consuming archaea revealed by directly coupled isotopic and phylogenetic analysis. Science 293, 484–487.
Orphan, V.J., House, C.H., Hinrichs, K.-U., McKeegan, K.D., DeLong, E.F., 2002. Multiple archaeal groups mediate methane oxidation in anoxic cold seep sediments. Proceedings of the National Academy of Sciences 99, 7663–7668.
Orpin, A.R., 1997. Dolomite chimneys as possible evidence of coastal fluid expulsion, uppermost Otago continental slope, southern New Zealand. Marine Geology 138, 51–67.
Ostwald, J., England, B.M., 1977. Notes on framboidal pyrite from Allandale New South Wales, Australia. Mineralium Deposita 12, 111–116.
Ostwald, J., England, B.M., 1979. The relationship between euhedral and framboidal pyrite in base metal sulphide ores. Mineral Magmatic 43, 297–300.
Pancost, R.D., Sinninghe Damsté, J.S., de Lint, S., van der Maarel, M.J., Gottschal, J.C., The Medinaut Shipboard Scientific Party, 2000. Biomarker evidence for widespread anaerobic oxidation in Mediterranean sediments by a consortium of methanogenic archaea and bacteria. Applied and Environmental Microbiology 66, 1126–1132.
Pancost, R.D., Hopmans, E.C., Sinninghe Damsté, J.S., The Medinaut Shipboard Scientific Party, 2001. Archaeal lipids in Mediterranean cold seeps: molecular proxies for anaerobic methane oxidation. Geochimica et Cosmochimica Acta 65, 1611–1627.
Paull, C.K., Neumann, A.C., 1987. Continental margin brine seeps: their geological consequences. Geology 15, 545–548.
Paull, C.K., Chanton, J.P., Neumann, A.C., Coston, J.A., Martens, C.S., Showers, W., 1992. Indicators of methane-derived carbonates and chemosynthetic organic carbon deposits: examples from the Florida Escarpment. Palaios 7, 361–375.
Paull, C.K., Ussler III, W., Borowski, W.S., Spiess, F.N., 1995. Methane-rich plumes on the Carolina continental rise: associations with gas hydrates. Geology 23, 89–92.
Paull, C.K., Schlining, B., Ussler III, W., Paduan, J.B., Caress, D., Greene, H.G., 2005. Distribution of chemosynthetic biological communities in Monterey Bay, California. Geology 33, 85–88.
Peckmann, J., Reimer, A., Luth, U., Luth, C., Hansen, B.T., Heinicke, C., Hoefs, J., Reitner, J., 2001. Methane-derived carbonates and authigenic pyrite from the northwestern Black Sea. Marine Geology 177, 129–150.
Pierre, C., Rouchy, J.M., Gaudichet, A., 2000. Diagenesis in the gas hydrate sediments of the Blake Ridge: mineralogy and stable isotope compositions of the carbonate and sulfide minerals. In: Paull, C.K., Matsumoto, R., Wallace, P.J., Dillon, W.P. (Eds.), Proceedings of the Ocean Drilling Program. Scientific Results, vol. 164. Ocean Drilling Program, College Station, Texas, pp. 139–146.
Ratnamohan, V.M., Cunningham, A.L., Rawlinson, W.D., Mukhopadhyay, P.K., Goodarzi, F., Crandlemire, A.L., Gillis, K.S., Macneil, D.J., Smith, W.D., 1998. Comparison of coal composition and elemental distribution in selected seams of the Sydney and Stellarton Basins, Nova Scotia, Eastern Canada. International Journal of Coal Geology 37, 113–141.
Rickard, D.T., Schoonen, M.A.A., Luther III, G.W., 1995. Chemistry of iron sulfides in sedimentary environments. In: Vairavamurthy, M.A., Schoonen, M.A.A. (Eds.), Geochemical Transformations of Sedimentary Sulphur. American Chemical Society Symposium Series, vol. 612, pp. 168–193.
Ritger, S., Carson, B., Suess, E., 1987. Methane-derived authigenic carbonates formed by subduction-induced pore-water expulsion along the Oregon/Washington margin. Geological Society of America Bulletin 98, 147–156.
Roberts, A.P., Jiang, W.T., Florindo, F., Horng, Ch.-S., Laj, C., 2005. Assessing the timing of greigite formation and the reliability of the Upper Olduvai polarity transition record from the Crostolo River, Italy. Geophysical Research Letters 32, doi:10.1029/2004GL022137.
Sassen, R., Roberts, H.H., Carney, R., Milkov, A.V., DeFreitas, D.A., Lanoile, B., Zhang, C., 2004. Free hydrocarbon gas, gas hydrate, and authigenic minerals in chemosynthetic communities of the northern Gulf of Mexico continental slope: relation to microbial processes. Chemical Geology 205, 195–217.
Sawlowicz, Z., 1987. Framboidal pyrite from the metamorphic Radzimowice Schists of Stara Gora (Lower Silesia, Poland). Mineralogia Polonica 18, 57–67.
Sawlowicz, Z., 1993. Pyrite framboids and their development: a new conceptual mechanism. Geologische Rundschau 82, 148–156.
Sawlowicz, Z., 2000. Framboids: from their origin to application. Prace Mineralogiczne 88, 1–80.
Schieber, J., Baird, G., 2001. On the origin and significance of pyrite spheres in Devonian black shales of North America. Journal of Sedimentary Research 71, 155–166.
Schoonen, M.A.A., 2004. Mechanisms of sedimentary pyrite formation. In: GSA Special Paper, vol. 379, pp. 117–134.
Shnukov, E.F., Sobolevskiy, Yu.V., Kutniy, V.A., 1995. Unusual carbonate buildups at continental slope of the north-western Black Sea – an apparent consequence of the degassing of sediments. Lithology and Minerals Resources. (Litologiya i Poleznye Iskopaemye, Moscow, Russia) 5, 461–541 (in Russian).
Somoza, L., Díaz-del-Río, V., León, R., Ivanov, M., Fernández-Puga, M.C., Gardner, J.M., Hernandez-Molina, F.J., Pinheiro, L.M., Rodero, J., Lobato, A., Maestro, A., Vázquez, J.T., Medialdea, T., Fernández-Salas, L.M., 2003. Seabed morphology and hydrocarbon seepage in the Gulf of Cádiz mud volcano area: acoustic imagery, multibeam and ultra-high resolution seismic data. Marine Geology 195, 153–176.
Stakes, D.S., Orange, D., Paduan, J.B., Salamy, K.A., Maher, N., 1999. Cold-seeps and authigenic carbonate formation in Monterey Bay, California. Marine Geology 159, 93–109.
Suess, E., Bohrmann, G., von Huene, R., Linke, P., Wallmann, K., Lammers, S., Sahling, H., Winckler, G., Lutz, R.A., Orange, D., 1998. Fluid venting in the eastern Aleutian subduction zone. Journal of Geophysical Research 103, 2597–2614.
Sweeney, R.E., Kaplan, I.R., 1973. Pyrite framboid formation: laboratory synthesis and marine sediments. Economic Geology 68, 618–634.
Taylor, G.R., 1982. A mechanism for framboid formation as illustrated by a volcanic exhalative sediment. Mineralium Deposita 17, 23–36.
Teichert, B.M.A., Bohrmann, G., Suess, E., 2005. Chemoherms on Hydrate Ridge – unique microbially-mediated carbonate build-ups growing into the water column. Palaeogeography, Palaeoclimatology, Palaeoecology 227, 67–85.
Teske, A., Hinrichs, K.-U., Edgcomb, V., de Vera Gomez, A., Kysela, D., Sylva, S.P., Sogin, M.L., Jannasch, H.W., 2002. Microbial diversity of hydrothermal sediments in the Guaymas Basin: evidence for anaerobic methanotrophic communities. Applied and Environmental Microbiology 68, 1994–2007.
Thiel, V., Peckmann, J., Seifert, R., Wehrung, P., Reitner, J., Michaelis, W., 1999. Highly isotopically depleted isoprenoids: molecular markers for ancient methane venting. Geochimica et Cosmochimica Acta 63, 3959–3966.
Thiel, V., Peckmann, J., Richnow, H.H., Luth, U., Reitner, J., Michaelis, W., 2001. Molecular signals for anaerobic methane oxidation in Black Sea seep carbonates and a microbial mat. Marine Chemistry 73, 97–112.
Thomsen, T.R., Finster, K., Ramsing, N.B., 2001. Biogeochemical and molecular signatures of anaerobic methane oxidation in a marine sediment. Applied and Environmental Microbiology 67, 1646–1656.
Valentine, D.L., 2002. Biogeochemistry and microbial ecology of methane oxidation in anoxic environments: a review. Antonie Van Leeuwenhoek 81, 271–282.
Valentine, D.L., Reeburgh, W.S., 2000. New perspectives on anaerobic methane oxidation. Environmental Microbiology 2, 477–484.
Whiticar, M.J., Werner, F., 1991. Pockmarks: submarine vents of natural gas or freshwater seeps? Geo-Marine Letters 1, 193–199.
Wilkin, R.T., Barnes, H.L., Brantley, S.L., 1996. The size distribution of framboidal pyrite in modern sediments: an indicator of redox conditions. Geochimica et Cosmochimica Acta 60, 3897–3912.
Wilkin, R.T., Barnes, H.L., 1997. Formation processes of framboidal pyrite. Geochimica et Cosmochimica Acta 61, 323–339.
Zhang, C.L., Li, Y., Wall, J.D., Larsen, L., Sassen, R., Huang, Y., Wang, Y., Peacock, A., White, D.C., Horita, J., Cole, D.R., 2002. Lipid and carbon isotopic evidence of methane-oxidizing and sulfate-reducing bacteria in association with gas hydrates from the Gulf of Mexico. Geology 30, 239–242.